Production of Hydroxy Fatty Acids and its Effects on Photosynthesis in the Cyanobacterium *Synechocystis* sp. PCC 6803

Takashi Inada[a], Shuntaro Machida[a,b], Koichiro Awai[c], Iwane Suzuki[d]

[a]*Graduate School of Life and Environmental Sciences, University of Tsukuba, Tennoudai 1-1-1, Tsukuba, Ibaraki 305-8572, Japan*

[b]*Food Research Institute, National Agriculture and Food Research Organization, Kannondai 2-1-12, Tsukuba, Ibaraki 305-8642, Japan*

[c]*Department of Biological Science, Faculty of Science, Shizuoka University, Shizuoka, Japan*

[d]*Faculty of Life and Environmental Science, University of Tsukuba, Tennoudai 1-1-1, Tsukuba, Ibaraki 305-8572, Japan*

[b]*Present affiliation: Department of Chemical and Biological Engineering, National Institute of Technology, Ube College 2-14-1 Tokiwadai, Ube, Yamaguchi 755-8555, Japan*

Abstract

Microalgal lipids and fatty acids are important components for achieving biofuel because of their potential high productivity. Although fatty acids that have a hydroxy group adjacent to the end of the acyl chain might be an important chemical feedstock, most algae do not accumulate it. To produce (ω-1)-hydroxy fatty acids from 3-hydroxybutylyl-CoA, an intermediate for polyhydroxybutylate biosynthesis in the cyanobacterium *Synechocystis* sp. PCC 6803, we expressed a gene for the promiscuous 3-ketoacyl-ACP synthase III from *Alicyclobacillus acidocalderius* (aaKASIII) by the *cpc560* promoter. To supply 3-hydroxybutyryl-CoAs for aaKASIII, the *phaC* gene for polyhydroxybutylate polymerase was deleted, and the *phaAB* genes for 3-hydroxybutyryl-CoA synthesis from *Cupriavidus necator* were overexpressed. The genetically modified strain synthesized 15-hydroxyhexadecanoic acid, 17-hydroxyoctadecanoic acid, and 17-hydroxyoctadec-9-enoic acid, and accumulated approximately 2.1 mol% of (ω-1)-hydroxy fatty acids in total fatty acids under

illumination with 70 μmol photons m^{-2} s^{-1}, although its growth was severely retarded. Under weak light (35 μmol photons m^{-2} s^{-1}) conditions, the strain grew as well as the wild-type and showed lower hydroxy fatty acids (0.04 mol%) accumulation than that at higher illumination levels. The photosynthetic activity of this strain was lower than that of wild-type cells, suggesting that high light conditions enhanced hydroxy fatty acids production and inhibited photosynthesis. (ω-1)-Hydroxy fatty acids were not predominantly observed in the galactolipids from thin-layer chromatography, which are the major lipid classes in cyanobacteria. To the best of our knowledge, this is the first report on photoautotrophic production of fatty acids possessing a functional group near the end of the acyl chain in cyanobacteria.

Keywords: 3-Ketoacyl-ACP Synthase III, Fatty acid synthesis, Bio-based chemicals, Omega-functionalized fatty acids, Metabolic engineering

1. Introduction

Recently, vegetable oils have become an important feedstock for chemicals as they contain lipids and fatty acids (FAs), which are not present in petroleum oil, and large amount of vegetable oils are produced worldwide [1] and used in the oleochemical industry for various applications. To expand the use of lipids and FAs from vegetable oils as raw materials, the synthesis of functionalized FAs by chemical and biotechnological engineering is essential. The hydroxy group is one of the most effective functional groups in the chemical reactivity of FAs, and its positions in the acyl chain play a vital role in its physiological mechanisms and chemical applications [2]. In particular, FAs that have a hydroxy group at the proximity of the ω-position of the acyl chain possess a high availability for various kinds of chemical feedstock, such as adhesives, lubricants, cosmetic intermediates [3], potential anticancer agents [4], and building blocks for the synthesis of polyesters, which exhibit similar or superior physicochemical properties to polyethylene and other bioplastics [5]. FAs with a hydroxy group near the ω-position are naturally produced in a wide variety of organisms [6–8], most of which synthesize these hydroxylated FAs through ω-oxidation by cytochrome

P450 monooxygenase. Whole-cell biocatalysis of the enzyme achieves a high conversion ratio of FA hydroxylation and shows great potential for large-scale production of industrial applications [9].

Microalgal oil is attracting attention as a resource of FA because microalgae have the potential to achieve high productivity, cultivate on non-arable land, grow in wastewater, and their cells can be modified by genetic engineering. Despite these advantages, FA from microalgae is a controversial technology because several issues remain before achieving economic competitiveness in the production process, i.e., collection of cells, drying of the cells, and FA extraction. The production of high-value compounds by microalgae is a potential solution to achieve economic competitiveness. As high-value products from microalgal oils, hydroxy FAs might be a possible candidate that could be applied for the feedstock of unique compounds. Recently, the genetically modified diatom *Chaetoceros gracilis,* with the FA dehydrogenase gene from ergot fungus *Claviceps purpurea*, produces ricinoleic acid (12-hydroxy-9-*cis*-octadecanoic acid) [10]. Despite the growth inhibition of yeast or other organisms owing to the production of hydroxy FAs, this diatom can produce ricinoleic acid without growth inhibition because detoxification of hydroxy FA naturally occurs by esterification of the hydroxy group with a carboxyl group on the other FAs. In this diatom, The detoxification mechanism and the effect of hydroxy FA on photosynthesis are unclear [11]. However, there are no studies either to produce FAs that contain a hydroxy group at the proximity of the ω-position by genetic engineering of microalgae or to investigate the effect of hydroxy FAs on photosynthesis.

Cyanobacteria is utilized as a model to investigate the function and mechanism of photosynthesis. A study on the cyanobacteria FAs is significant in terms of FA production and physiological analysis. For free FA production, overproduction and secretion of free FAs are achieved in cyanobacterial strains by genetic manipulations [12–14]. In addition, to obtain cyanobacterial cells that are oxidation-tolerant and maintain the fluidity of membrane lipids, we succeeded in producing FAs such as cyclopropane FAs and 10-methyl stearic acid in transformants of *Synechocystis* sp. PCC 6803 (hereafter *Synechocystis*) [15,16]. These results indicate that cyanobacteria are a promising organism for application in the modification to produce unnatural FAs. A thorough study on the relationship between FA and photosynthetic pigment in *Synechocystis* can help understand the effects of hydroxy FA production on photosynthesis, which has never been investigated.

Regarding biochemical synthesis, cyanobacteria mainly produce glycolipids, i.e., monogalactosyldiacylglycerol (MGDG) and digalactosyldiacylglycerol (DGDG) as the major lipid components, while *Escherichia coli* and *Rhodospirillum rubrum,* which are host organisms for the production of hydroxy FAs in this study, mainly synthesize phospholipids. Glycolipids with hydroxy FAs have the potential to be utilized as novel glycolipid biosurfactants [17].

In this study, we attempted to synthesize (ω-1)-hydroxy fatty acids (ω1HFAs) in the cyanobacterium *Synechocystis* by genetic engineering. *Synechocystis* synthesizes 3-hydroxybutyryl-CoA (3HB-CoA) as a metabolic intermediate in the synthesis of polyhydroxybutyrate (PHB). If 3HB-CoA is incorporated into the *de novo* synthesis pathway of FA instead of acetyl-CoA, it might produce ω1HFAs. To achieve this, the substrate flexibility of β-ketoacyl-ACP-synthase III (KASIII), which is the enzyme for the first reaction of the fatty acid synthesis pathway, is attractive. The reaction by KASIII defines the chemical structure of the ω-end of FAs by the structure of the acyl-CoA moiety and substrate specificity of KASIII. In general, KASIII uses acetyl-CoA as a substrate. KASIII from *Alicyclobacillus* (aaKASIII) uses alicyclic acyl-CoA instead of acetyl-CoA, and its specific activity for the reaction between 3HB-CoA and malonyl-ACP is 3-fold higher than that for the reaction between acetyl-CoA and malonyl-ACP [18]. This feature of aaKASIII is good for 3HB-CoA as a substrate. For 3HB-CoA biosynthesis, PhaAB from *Cupriavidus necator* H16 (CPhaAB) is one of the best enzymes in *Synechocysitis*. In previous studies, CphaAB showed much higher activity than other enzymes for overproduction of PHB or 3-hydroxybutyrate in engineered cyanobacteria and did not show growth inhibition [19,20]. An engineered *E. coli* strain*,* with the promiscuous KASIII and 3HB-CoA synthesis pathway, produces ω1HFAs [18]. Thus, we adapted this strategy for the production of ω1HFAs in *Synechocystis*.

2. Materials and Methods

2.1 Organisms and culture conditions

In this study, a glucose-tolerant strain of *Synechocystis* [21] was used as the wild-type strain. *Synechocystis* cells were grown in BG11 medium [22] buffered with 20 mM 4-(2-hydroxyethyl)-1-piperazineethanesulfonic acid (HEPES)–NaOH (pH 7.5) at 34 °C under continuous illumination by white fluorescent lamps and aerated with 1% (v/v) CO_2-enriched air [23]. Fifty milliliters of cultures were used for measurement of growth, FA compositions, and mixotrophic culture, and 500 mL of cultures were used for simultaneous measurement of ω1HFAs and photosynthetic parameters.

To screen the transformants and maintain the *Synechocystis* cells, we used BG11 medium solidified with 1.5% (w/v) Bacto-agar (BD Biosciences Japan, Tokyo, Japan), including 25 μg mL^{-1} kanamycin sulfate or chloramphenicol (Fujifilm Wako Pure Chemical, Osaka, Japan), depending on the selection markers. An *E. coli* strain JM109 [24] was grown in 1.8 mL of LB medium [25] at 37 °C with shaking at 180 rpm. All transformants of *E. coli* were maintained on LB medium solidified with 1.5% (w/v) Bacto-agar in the presence of 100 μg mL^{-1} sodium ampicillin (Fujifilm Wako Pure Chemical) and 50 μg mL^{-1} kanamycin sulfate or chloramphenicol, depending on the selection markers.

2.2 Plasmid construction and transformation

The scheme for constructing plasmids in this study is summarized in Fig. S1. To express the heterologous promiscuous KASIII gene and knockout the *fabH* gene, which encodes a native KASIII in *Synechocystis*, we constructed a plasmid, pMD19Δ*fabH::aaKASIII*. We performed PCR to amplify a DNA fragment containing *aaKASIII* using the chromosomal DNA of *Alicylobacillus acidocalderius* subsp. *acidocalderius* JCM 5260^T (RIKEN BRC, Ibaraki, Japan) as the template and the primer set aaKASIII_F and aaKASIII_R (Table S4). After digestions of pTC2031 [15] and the amplified fragment containing the aaKASIII gene with *Nde*I and *Bgl*II, we constructed pTC2031_aaKASIII by ligation. The genomic fragments corresponding to the *fabH* gene were amplified by PCR using *Synechocystis* chromosomal DNA as the template and primer set fabH_up_F and fabH_dn_R. The amplified DNA fragment was subcloned into a T-vector pMD19 simple vector (Takara Bio, Kusatsu, Japan) to obtain the plasmid pMD19_fabH. To obtain plasmid pMD19Δ*fabH::aaKASIII*, pMD19_*fabH* was linearized by PCR using the primer set fabH_in_F and

fabH_in_R, and ligated with the *CmR-Pcpc-aaKASIII* fragment using pTC2031_aaKASIII plasmid as the template and primer set CmCK_inf_F and CmCK_inf_R using the In-Fusion® HD cloning kit (Takara Bio).

To construct pMD19Δ*phaC*, which is used to knock out the *phaC* gene for PHB polymerase, we performed PCR to amplify a DNA fragment containing *phaC* using *Synechocystis* chromosomal DNA as the template and the primer set phaC_up_F and phaC_dn_R. The amplified DNA fragment was subcloned into a T-vector pMD19 simple vector to obtain the plasmid pMD19_*phaC*. To obtain plasmid pMD19 Δ*phaC*, pMD19_*phaC* was linearized by PCR using the primer set phaC_in_F and phaC_in_R, and circularized with the DNA fragments corresponding to the kanamycin-resistance gene cassette, EZ-Tn5 < KAN-2 > Tnp Transposome Kit (Epicenter, Madison WI) using primer sets Kam_inf_F and Kam_inf_R with the In-Fusion® HD cloning kit.

To construct pMD19_*ΔphaC::SphaAB* for overexpression of the *phaAB* gene from *Synechocystis* and knockout the *phaC* gene in *Synechocystis*, we performed PCR to amplify a DNA fragment containing *phaAB* using *Synechocystis* chromosomal DNA as the template, and the primer sets phaAB_up_F and phaAB_dn_R. After digestion of pTC2031 and the amplified fragment containing *SphaAB* with *Nde*I and *Bgl*II, we constructed pTC2031_*SphaAB* by ligation. To construct pMD19*ΔphaC::SphaAB*, pMD19*ΔphaC* was linearized by PCR using primer sets pMD19_Km_PhaC_in_F and pMD19_Km_PhaC_in_F, and ligated with the DNA fragment *Pcpc-phaAB* using pTC2031_*SphaAB* as the template and the primer set cpc_phaAB_inf_F and cpc_phaAB_inf_R with the In-Fusion® HD cloning kit.

To construct pMD19Δ*phaC::CphaAB,* which is a plasmid for overexpression of the heterologous *phaAB* genes from *Cupriavidus necator* H16 (RIKEN BioResource Center) at the *phaC* locus by homologous recombination, pMD19Δ*phaC::SphaAB* was linearized by PCR using primer sets pMD19_Km_PhaC_in_F and cpc560_R, and ligated with the *CphaAB* fragment using *C. necator* H16 chromosomal DNA as the template and the primer sets CphaAB_inf_F and CphaAB_inf_R by the In-Fusion® HD cloning kit.

To construct pTC2031-S_sodB*,* that is a plasmid for overexpression of the *sodB* gene from *Synechocystis* at the *slr2031* locus by homologous recombination, pTC2031-S [15] was linearized by PCR using primer set

pTCS_Sp_up_F and cpc560_R, and ligated with the *sodB* fragment using *Synechocystis* chromosomal DNA as the template and the primer set sodB_inf_F and sodB_inf_R by the In-Fusion® HD cloning kit.

The DNA sequences of the inserts were confirmed using BigDye® Terminator v.3.1 (Life Technologies, Foster City, CA, USA) and ABI 3130 Genetic Analyzer (Life Technologies).

2.3 FA analysis

The FA profiles of *Synechocystis* transformants were examined using the methods described in our previous studies [15,16,26]. Cells were precipitated by centrifugation, resuspended in 2 mL of methanol, and transferred to glass test tubes. After thorough drying using a concentrating centrifuge (CC-105, Tomy Seiko, Tokyo, Japan), the residue was resuspended in 0.1 M hydrochloric acid methanolic solution (Fujifilm Wako Pure Chemical). The tubes were tightly capped and incubated at 100 °C for 1 h to allow for methyl esterification of the acyl groups in the lipids and conversion into FA methyl esters. The resulting FA methyl esters were extracted using *n*-hexane. The recovered hexane phases were evaporated, and the residues containing FA methyl esters were dissolved in 100 μL of acetonitrile and trimethylsilylated by adding 100 μL of *N*, *O*-bis(trimethylsilyl)acetamide: pyridine (1:1), and heated at 90 °C for 30 min. The trimethylsilylation of the hydroxy group in the acyl group contributes to the separation of FA methyl esters by decreasing the evaporation temperature and easily identifying the fragmentation of FA methyl esters [27,28]. To identify FA methyl esters, we performed gas chromatography (GC) using a GC-2010 gas chromatograph equipped with a QP-2010 mass spectrometer (Shimadzu, Kyoto, Japan). Helium was used as a carrier gas at a constant flow rate of 1.25 mL min^{-1} in split-less mode. A CP-Sil5 CB column (Agilent Technologies, Santa Clara, CA, USA) was used at the following temperatures: 60 °C for 1.5 min, followed by 130 °C at a rate of 20 °C min^{-1}, and then a further increase to 230 °C at a rate of 4 °C min^{-1}.

2.4 Separation of lipid classes

To analyze FAs attached to each lipid, the harvested cells were dried using a freeze dryer, and the lipids were extracted with $CHCl_3$: methanol (2:1, v/v). The cell debris was sedimented by centrifugation. The

resulting supernatant was transferred into new tubes and evaporated. Then, the samples were resuspended in 500 μL of $CHCl_3$:methanol (2:1, v/v) and applied to a silica gel plate (silica gel 70 FM TLC Plate- Wako, 20 cm × 20 cm; Fujifilm Wako Pure Chemical) washed with $CHCl_3$:methanol (1:1, v/v). Lipids were separated by thin-layer chromatography using acetone:toluene:water (91:30:8, v/v/v). In particular, when plenty of lipids were applied on the thin-layer chromatography (TLC) plates to improve the separation of lipid species, we repeated the development of the solvent at most three times. The lipids were stained with primulin, and the silica gel corresponding to the lipid spots was then scraped off and extracted as described above. To identify the head group of lipid X, the TLC plate was visualized with α-naphthol [29]. The lipids on the TLC plate were stained by spraying 0.2 M α-naphthol in ethanol: 75% (w/v) H_2SO_4aq (4:11, v/v) and heated at 120 °C for 10 min [30].

2.5 Lipid analysis by liquid chromatography-mass spectrometry

For liquid chromatography-mass spectrometry (LC-MS) analysis, separation by high-performance liquid chromatography was carried out using a Prominence XR (Shimadzu). The sample was analyzed using L-column2 ODS Nonmetallic frits (2 mm I.D. × 50 mm, 3 μm, Chemical Evaluation and Research Institute, Tokyo, Japan). The liquid separation phases were prepared by mixing three solvents. Solvents A, B, and C were 1 mM ammonium formate, acetonitrile, and 1 mM ammonium formate in 2-propanol, respectively. The gradient profile was as follows: (i) initial 60% A + 38% B + 2% C; (ii) 30 min linear gradient to 2% A + 10% B + 88% C; (iii) 38 min isocratic; (iv) 38.1 min 60% A + 38% B + 2% C; and (v) 41.0 min isocratic. The flow rate was 0.3 mL min^{-1}, and the column temperature was 40 °C. The injection volume was 3 μL. An LTQ Orbitrap XL (Thermo Fisher Scientific) mass spectrometer was operated in both positive and negative ion modes with an electrospray ionization source in the range of *m/z* 140−2000. Xcalibur ver. 2.1.0 (Thermo Fisher Scientific) was used to process and analyze the data.

2.6 Measurement of photosynthetic activities

Chlorophyll was extracted in 90% methanol and calculated by measuring the absorbance at 665 nm [31]. The oxygen evolution rate of intact cells was measured with a Clark-type oxygen electrode (Oxytherm System, Hansatech Instruments, Norfork, UK). Cells were suspended in BG-11 medium containing 20 mM $NaHCO_3$, and photosynthetic activity in the samples was measured at a light intensity of 300 μmol photons m^{-2} s^{-1}, which represented saturated light conditions. The photosynthetic yield of PSII was determined by measuring the Fv/Fm ratio using an AquaPen fluorometer (AP 100, Photon Systems Instruments, Drasov, Czech). Samples were dark-adapted for 5 min before measurement.

3 Results and Discussion

3.1 Construction of the hydroxy FA synthetic pathway and analysis of the FAs in transformants

To introduce 3HB-CoA into the FA synthesis pathway in *Synechocystis* cells, we utilized a substrate-variable β-keto-acyl-(acyl carrier protein) synthase III (KASIII), which catalyzes the condensation of acetyl-CoA and malonyl-ACP at the first reaction of the FA synthesis pathway. KASIII from *A. acidocalderius* (aaKASIII) has a very wide substrate specificity [18], which can react with many types of acyl-CoA, e.g., propionyl-CoA, isobutyryl-CoA, and benzoyl-CoA, as substrates instead of acetyl-CoA. *E. coli* transformants, which express the aaKASIII and 3HB-CoA biosynthetic gene cluster, produced ω1HFAs [18] (Fig. 1). *Synechocystis* can synthesize 3HB-CoA, which is a precursor of PHB for carbon storage. To incorporate 3HB-CoA synthesized in *Synechocystis* cells into the FA synthesis pathway, the *fabH* gene encoding the native KASIII of *Synechocystis* was replaced with the aaKASIII gene. This *Synechocystis*Δ*fabH*::*aaKASIII* strain (*aaKASIII*+) was cultivated under photoautotrophic conditions with the standard BG-11 medium [22] for 7 d. GC-MS analysis revealed that the transformant under the standard BG-11 condition contained no ω1HFAs. We speculated that the 3HB-CoA pool in *Synechocystis* cells cultivated under standard BG-11 conditions was not sufficient to synthesize ω1HFAs because of the low PHB accumulation, i.e., approximately 1%−5% (w/w) of dry cells.

To increase the content of 3HB-CoA, two additional genetic modifications were employed. First, the ability of PHB polymerization was deleted because PHB synthesized from 3HB-CoA should compete with ω1HFA biosynthesis. Because PHB biosynthesis from 3HB-CoA is catalyzed by PHB polymerase encoded by the *phaC* and *phaE* genes, we inactivated the *phaC* gene to enhance the accumulation of 3HB-CoA, the ω1HFA precursor. Second, we overexpressed *phaA* and *phaB* (*phaAB*) genes by substituting with the *phaC* gene in the cells of *aaKASIII*+. These two gene products are involved in the biosynthesis of 3HB-CoA, PhaA catalyzes the condensation of two acetyl-CoA molecules to yield acetoacetyl-CoA, and PhaB then reduces it to 3HB-CoA. In addition to *Synechocystis*Δ*fabH*::*aaKASIII*, we constructed two other transformants, Δ*phaC* (*aaKASIII*+/*phaC*−), *Synechocystis*Δ*fabH*::*aaKASIII*, Δ*phaC*::*SphaAB* (*aaKASIII*+/*phaC*−/*SphaAB*+). However, ω1HFAs were not detected in either *aaKASIII*+/*phaC*− and *aaKASIII*+/*phaC*−/*SphaAB*+ cells cultivated in the standard BG-11. To enhance 3HB-CoA biosynthesis, we cultivated *aaKASIII*+, *aaKASIII*+/*phaC*−, and *aaKASIII*+/*phaC*−/*SphaAB*+ cells under phosphate-limiting conditions with 4% acetate, and PHB productivity was increased up to 28.8% (w/w) of the dry cells [32]. However, under photomixotrophic conditions, the FA composition extracted from these transformants showed no ω1HFAs (data not shown).

To further increase 3HB-CoA biosynthesis, we attempted to express the exogenous *phaAB* genes in *Synechocystis*. In a previous study [43], PhaA and PhaB from *C. necator* H16 had much higher activity than those in *Synechocystis*. We introduced the *phaAB* genes of *C. necator* H16 into the *phaC* region of *Synechocystis*Δ*fabH*::*aaKASIII* strain to obtain *Synschocystis*Δ*fabH*::*aaKASIII*, Δ*phaC*::*CphaAB* (*aaKASIII*+/*phaC*−/*CphaAB*+) cells. Total lipids were extracted from the *aaKASIII*+/*phaC*−/*CphaAB*+ cells cultivated under standard BG-11 conditions with 70 μmol photons m^{-2} s^{-1} illumination, and then trans-esterified and trimethylsilylated. The total ion chromatogram of FA methyl esters from the *aaKASIII*+/*phaC*−/*CphaAB*+ cells showed three additional peaks, **1**, **2**, and **3**, with retention times of 25.1, 28.5, and 29.2 min, respectively, compared to that of wild-type cells (Fig 2A). As the canonical ω1HFAs were not commercially available, we had to identify them from the fragment patterns by GC/MS analyses. The fragmented ions from the three peaks contained a characteristic ion with *m/z* 117, which represents the

resultant ions from the ω1HFAs by α cleavage. Peaks **1**, **2**, and **3** also contained fragment ions, whose *m*/*z* corresponded to the loss of the ω methyl and methoxy groups (Fig. S1). The mass spectrometry of the three peaks corresponded to those of previous studies [18,33]. We determined that the three species of ω1HFAs were 15-hydroxyhexadecanoic acid (16:0 OH), 17-hydroxyoctadecanoic acid (18:0 OH), and 17-hydroxyoctadec-9-enoic acid (18:1 OH) (Fig. 2B and S2). These ω1HFAs might be chiral compounds because 3HB-CoA synthesized by PhaAB from *C. necator* H16 is (*R*)-3HB-CoA [20]. The ω1HFAs content was about 2.1 mol% of total FAs (Fig. 2). Interestingly, lipids in the *aaKASIII+*/*phaC−*/*CphaAB+* cells contained a high amount of 18:0 while decreasing the content of 18:2 and 18:3. We do not know about the relationship between ω1HFA production and the unsaturation alteration of C18 FAs. These results indicated that the higher enzyme activity of PhaAB from *C. necator* H16 allowed the synthesis of ω1HFAs in the engineered *Synechocystis* cells expressing the aaKASIII, which can catalyze 3HB-CoA as a substrate.

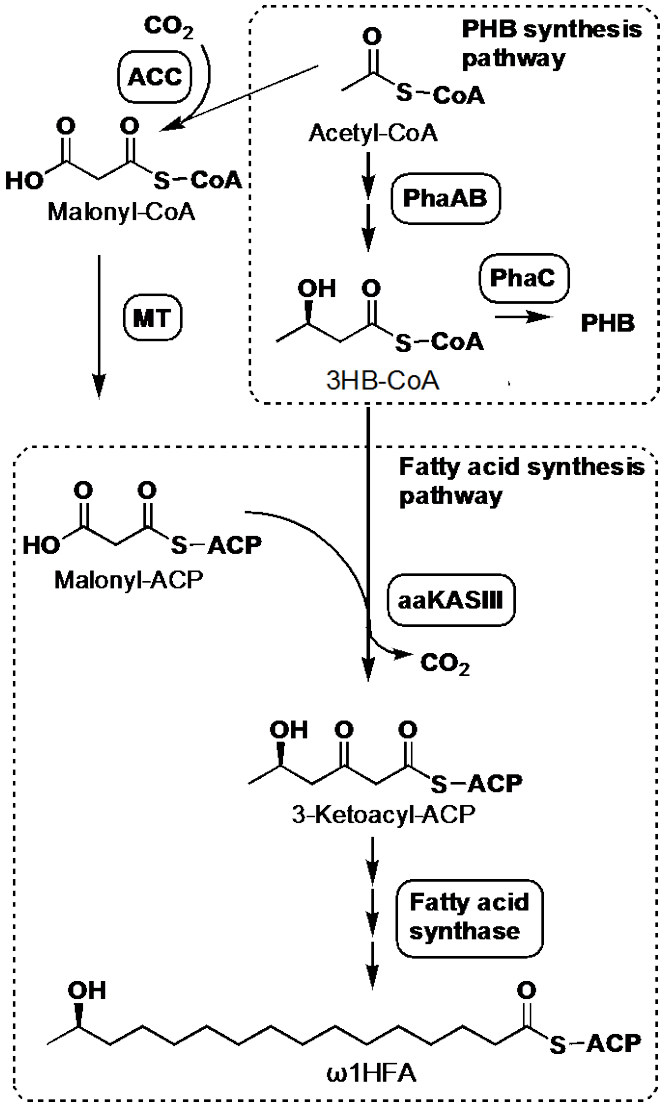

Fig. 1 (ω-1)-Hydroxy fatty acid (ω1HFA) production pathway. 3-Hydroxybutyryl-CoA (3HB-CoA) is synthesized from acetyl-CoA via a two-step reaction of the enzymes PhaA and PhaB. PHB is synthesized from 3HB-CoA by PhaC and PhaE. ω1HFAs were synthesized from 3HB-CoA introduced into the fatty acid synthesis pathway by catalyzing aaKASIII in a *Synechocystis* with deleted PhaC activity. ACC, MT, PHB, and ACP indicate acetyl-CoA carboxylase, malonyl coenzyme A-acyl carrier protein transacylase, polyhydroxybutyrate, and the acyl carrier protein, respectively.

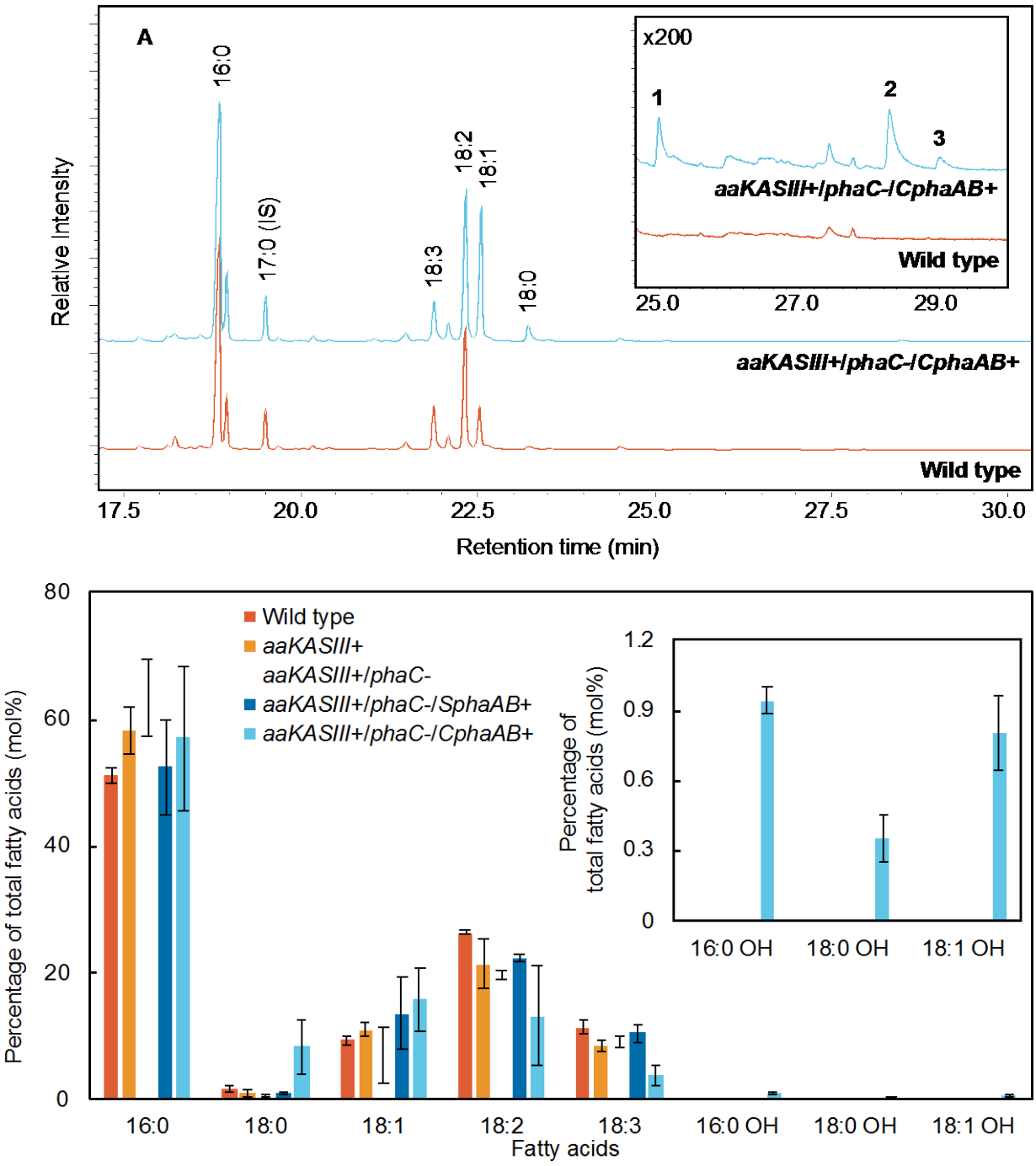

Fig. 2 (A) Gas chromatogram of fatty acid methyl esters from the lipids extracted from wild-type cells (red), and *aaKASIII+/phaC−/CphaAB+*; the cells in which the *fabH* gene was substituted with the *KASIII* gene from *Alicylobacillus acidocalderius* and the *phaC* gene was substituted with the *phaAB* genes from *Cupriavidus necator* H16 driven by the *cpc* promoter (pale-blue). (B) (ω-1)-Hydroxy fatty acid (ω1HFA) production in wild-type (red) and genetically engineered cells. Abbreviations of each genetically engineered cells are as follows: *aaKASIII+*; the cells in which the *fabH* gene was substituted with the *KASIII* gene from

Alicylobacillus acidocalderius (orange), *aaKASIII+*/*phaC−*; the *aaKASIII+* cells in which the *phaC* gene was inactivated (green), *aaKASIII+*/*phaC−*/*SphaAB+*; the *aaKASIII+* cells in which the *phaC* gene was substituted with the *phaAB* genes driven by the *cpc* promoter (blue), and *aaKASIII+*/*phaC−*/*CphaAB+*; the *aaKASIII+* cells in which the *phaC* gene was substituted with the *phaAB* genes from *Cupriavidus necator* H16 driven by the *cpc* promoter (pale-blue). 16:0, 18:0, 18:1, 18:2, 18:3, 16:0 OH. 18:0 OH, and 18:1 OH indicate palmitic, stearic, oleic, linoleic, γ-linolenic, 15-hydroxyhexadecanoic, 17-hydroxyoctadecanoic, and 17-hydroxyoctadec-9-enoic acid, respectively. Each data point represents an average of three independent experiments, and the error bars indicate the standard deviations.

3.2 Effects of hydroxy FA production on growth and photosynthesis.

Although all other strains constructed in this study grew as well as the wild-type under continuous illumination with 70 μmol photons m^{-2} s^{-1}, the growth of *aaKASIII+/phaC−/CphaAB+* cells was retarded. Interestingly, *aaKASIII+/phaC−/CphaAB+* cell growth under 35 μmol photons m^{-2} s^{-1}, was similar to that of wild-type cells (Fig. 3). However, under low-light conditions, *aaKASIII+/phaC−/CphaAB+* cells accumulated only a small amount of ω1HFAs (i.e., 0.04 mol%), which was much lower than that of cells grown under 70 μmol photons m^{-2} s^{-1} (Fig. S3). These results demonstrated the correlation between growth and ω1HFA biosynthesis in *Synechocystis* cells.

To investigate the relationship between ω1HFA production and photosynthesis, we simultaneously measured ω1HFA contents, photosynthetic activity, chlorophyll content, and photosynthetic yield of photosystem II (PSII) in the cells cultured under various light conditions, i.e., 35, 70, or 140 μmol photons m^{-2} s^{-1}, for 48 h. As a control, wild-type cells were cultivated under 140 μmol photons m^{-2} s^{-1} (Fig. 4). These measurements showed three important findings regarding the relationship between ω1HFA production and photosynthesis. First, the higher light intensity of cultivation stimulated ω1HFA accumulation in *Synechocystis* cells. Second, ω1HFA accumulation started in the early stage of cultivation. As high light intensity promoted the accumulation of acetyl-CoA, which stimulated of 3HB-CoA biosynthesis, ω1HFAs contents in *aaKASIII+/phaC−/CphaAB+* cells grown under 70 and 140 μmol photons m^{-2} s^{-1} rapidly increased within 6 h, while that of the cells cultivated at 35 μmol photons m^{-2} s^{-1} accumulated slowly (Fig. 4A). In particular, cells in the low cell density in the early stage of cultivation effectively absorbed photons and synthesized 3HB-CoA via acetyl-CoA biosynthesis. Third, ω1HFA accumulation in the early stage of cultivation inhibited photosynthesis activity under high light intensity. Under 140 μmol photons m^{-2} s^{-1}, photosynthetic parameters of *aaKASIII+/phaC−/CphaAB+* cells, i.e., chlorophyll content and quantum yield, Fv/Fm, continuously decreased after cultivation, while they maintained their initial levels under 35 and 70 μmol photons m^{-2} s^{-1}, with wild-type cells as a control (Fig. 4B and C). These changes in photosynthetic parameters suggested that ω1HFA accumulation in the early stage of cultivation promoted the inactivation of photosynthetic activity, i.e., photoinhibition. Under 140 μmol photons m^{-2} s^{-1},

aaKASIII+/*phaC−*/*CphaAB+* photosynthetic activity also dropped after 12 h and reached 26 μmol O_2 mg Chl^{-1} h^{-1} at 48 h. Meanwhile, under 35 μmol photons m^{-2} s^{-1}, it was maintained at approximately 60 μmolO_2 mg Chl^{-1} h^{-1} until 48 h (Fig. 4D). *aaKASIII+*/*phaC−*/*CphaAB+* cells incubated under 70 μmol photons m^{-2} s^{-1} and wild-type cells incubated under 140 μmol photons m^{-2} s^{-1} for 48 h reached approximately 50 and 60 μmolO_2 mg Chl^{-1} h^{-1}, respectively, owing to the apparent decrease in light intensity by self-scattering caused by the increase in cell density (Fig. 4D and Fig. S4). ω1HFA production in *aaKASIII+*/*phaC−*/*CphaAB+* cells incubated under 140 μmol photons m^{-2} s^{-1} reached 1.5 ± 1.3 mol% in total FAs at 24 h. These results indicate that ω1HFAs production, i.e., accumulation of membrane lipids esterified the ω1HFAs, caused a reduction in growth rate and photosynthetic activity.

3.3 Production of hydroxy FAs under mixotrophic conditions

To enhance ω1HFA production, *aaKASIII+*/*phaC−*/*CphaAB+* cells were cultivated for 1 day under mixotrophic conditions by addition of 10 mM glucose as a carbon source into BG-11 with continuous illumination at 140 μmol photons m^{-2} s^{-1}, and the initial cell density OD_{730} was 1.0 to protect the cells from inactivation of photosynthesis by high light intensity. Under this mixotrophic condition, *aaKASIII+*/*phaC−*/*CphaAB+* cells died, while under autotrophic conditions, the cells could survive and accumulated 1.9 mol% ω1HFA. Under heterotrophic conditions, i.e., cultured in the dark and adding 10 mM glucose, *aaKASIII+*/*phaC−*/*CphaAB+* cells could grow slowly but accumulated undetectable levels of ω1HFA (data not shown). The cells of *aaKASIII+* grown under the photomixotrophic conditions also grew slowly, suggesting that the knock-out of the native *fabH* gene might affect the glucose tolerance in *Synechocystis*.

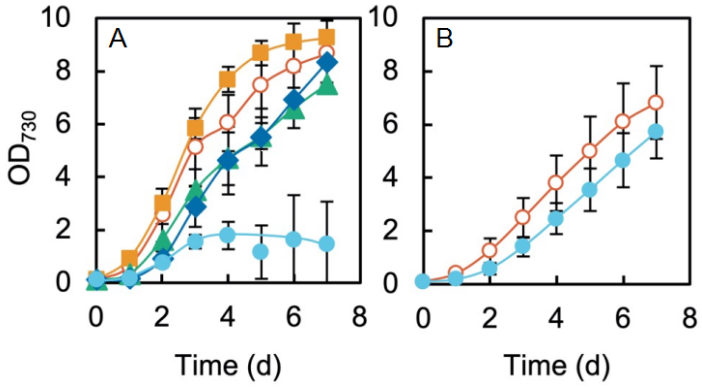

Fig. 3 Growth of the wild-type and recombinant cells of *Synechocystis*. (A) Growth of the wild-type (red open circle), *aaKASIII+*; the cells in which the *fabH* gene was substituted with the *KASIII* gene from *Alicylobacillus acidocalderius* (orange square), *aaKASIII+/phaC−*; the *aaKASIII+* cells in which the *phaC* gene was inactivated (green triangle), *aaKASIII+/phaC−/SphaAB+*; the *aaKASIII+* cells in which the *phaC* gene was substituted with the *phaAB* genes driven by the *cpc* promoter (blue diamond), and *aaKASIII+/phaC−/CphaAB+*; the *aaKASIII+* cells in which the *phaC* gene was substituted with the *phaAB* genes from *Cupriavidus necator* H16 driven by the *cpc* promoter (pale-blue circle) were cultivated under 70 μmol m^{-2} s^{-1}. (B) Growths of the wild type and *aaKASIII+/phaC−/CphaAB+* cells cultivated under 35 μmol m^{-2} s^{-1} were indicated by open and closed circles, respectively. OD_{730} indicate optical density at 730 nm. Each data point represents an average of three independent experiments, and the error bars indicate the standard deviations.

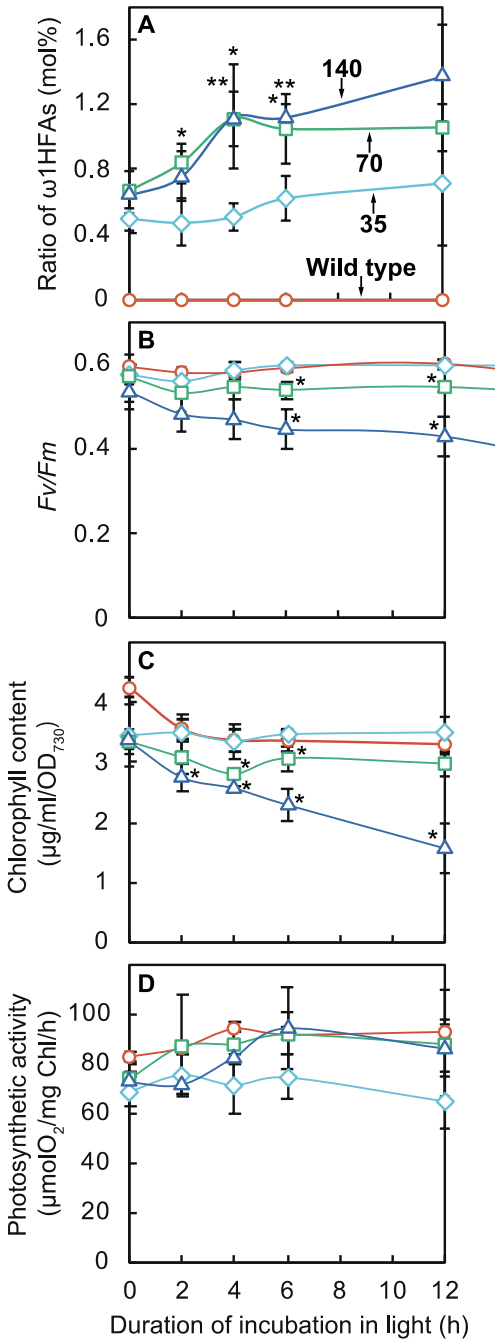

Fig. 4 (A) Effects of light intensity on (ω-1)-hydroxy fatty acids (ω1HFAs) production, (B) photosynthetic yield, (C) chlorophyll content, and (D) photosynthetic O_2-evolving activity of the *aaKASIII+/phaC−/CphaAB+*, the cells in which the *fabH* gene was substituted with the *KASIII* gene from *Alicylobacillus acidocalderius*, and the *phaC* gene was substituted with the *phaAB* genes from *Cupriavidus necator* H16 driven by the *cpc* promoter, grown under 35, 70, and 140 μmol photons m^{-2} s^{-1} (pale-blue diamonds, green squares, and blue triangles, respectively) and wild-type grown under 140 μmol photons m^{-2} s^{-1} (red circles). OD_{730} indicates optical density at 730 nm. Each data point represents an average of three

independent experiments, and the error bars indicate the standard deviations. Asterisks indicate significant differences with the parameters of *aaKASIII+*/*phaC−*/*CphaAB+* cells under 35 μmol photons m^{-2} s^{-1} (*P < 0.05, **P < 0.02, Student's t-test).

3.4 Lipid composition of the ω1HFA-producing transformant

The simultaneous measurement of ω1HFAs production and photosynthetic parameters indicated that ω1HFAs depressed photosynthesis. To understand the inactivation of photosynthesis by ω1HFAs in *aaKASIII+/phaC−/CphaAB+* cells, we measured ω1HFAs accumulation in each lipid class from *aaKASIII+/phaC−/CphaAB+* cells to analyze membrane lipids of the cells. Lipids were extracted from the wild-type and *aaKASIII+/phaC−/CphaAB+* cells and separated by TLC. Cyanobacteria have four classes of membrane lipids: MGDG, DGDG, sulfoquinovosyldiacylglycerol (SQDG), and phosphatidyldiacylglycerol (PG). Table 1 shows the FA compositions of all lipid classes from *aaKASIII+/phaC−/CphaAB+* cells, which were cultivated for 24 h under 70 μmol photons m^{-2} s^{-1} and accumulated 1.3 mol% ω1HFAs, with wild-type cells as a control. Total ω1HFAs in SQDG and PG extracted from the *aaKASIII+/phaC−/CphaAB+* cells were 0.8 and 0.9 mol%, respectively. The introduction of ω1HFAs into PG could explain the effect of ω1HFAs on photosynthetic activity and altering the growth rate because PG is directly bound to the photosystems and has a specific role in electron transport [34,35]. In particular, the hydroxy group of the ω1HFAs on PG, which is deeply buried in the reaction center of PSII, might be oxidized and cause structural disorder of PSII. The photosystem affected by ω1HFAs stimulates the production of reactive oxygen species that are toxic to the cells. To reduce reactive oxygen species in the *aaKASIII+/phaC−/CphaAB+* cells, we overexpressed the native superoxide dismutase which is a reactive oxygen species quenching enzyme encoded by *sodB* gene [36,37]. This *aaKASIII+/phaC−/CphaAB+/sodB+* strain grew better than *aaKASIII+/phaC−/CphaAB+* strain (Fig. S5), although *aaKASIII+/phaC−/CphaAB+/sodB+* strain produced same ratio of ω1HFA with *aaKASIII+/phaC−/CphaAB+* strain under 140 μmol photons m^{-2} s^{-1}. The decrease in Fv/Fm observed in *aaKASIII+/phaC−/CphaAB+* cells cultivated under 140 μmol photons m^{-2} s^{-1} was consistent with this hypothesis (Fig. 4B). Although galactolipids MGDG and DGDG were recovered from the TLC plates, they contained a small amount of ω1HFAs. Total lipids extracted from *aaKASIII+/phaC−/CphaAB+* cells showed an additional spot migrated under the spot of MGDG on the TLC plate, referred to as lipid X (Fig. 5). Visualization of lipid X on the TLC plate by α-naphthol turned the spot

of the lipid into yellow, indicating that the head group of lipid X might be a saccharide (Fig. S6). These staining results of lipid X on the TLC plate indicated that lipid X might be an MGDG analog.

To understand the small amount of ω1HFAs in galactolipids, we attempted to determine the molecular structure of lipid X by liquid chromatography coupled with mass spectrometry (LC-MS). We confirmed that lipid X included at least five species of galactolipids esterifying ω1HFA by the fragmentation pattern of LC/MS analyses, with the positive and negative ionization modes. The chromatogram of lipid X with the positive ionization mode indicated that lipid X was the mixture of at least five forms of lipids, which were separated at 19.25, 20.07, 21.06, 21.57, and 22.23 min, designated as peak No. **1**, **2**, **3**, **4**, and **5**, respectively (Fig. 5B and Fig. S7). As seen in Table S1, the mass spectra of these five lipids showed that all of them possessed major peaks between *m/z* 791.52 and 797.57, and minor peaks between *m/z* 807.50 and 813.54. The former might correspond to the parent lipid ionized with a sodium ion, $[M+Na]^+$, and the latter indicated potassium ionized from $[M+K]^+$. These peaks also contained five fragment ions, designated as **a**, **b**, **c**, **d**, and **e**, whose cleavage patterns are shown in Fig. 5D and Fig. S7A and B. Fragmentation was estimated from the reference MS data of MGDG from previous studies [38–40]. Structure estimation for the five lipid forms from the mass spectrum indicated that peaks No. **1**, **2**, **3**, **4**, and **5** were glycerolipids with a hexose ($C_6H_{12}O_6$) moiety as a headgroup, an ω1HFA, and either a saturated or unsaturated FA. The FA pairs of lipids, **1**, **2**, **3**, **4**, and **5** were estimated as 16:0 OH/18:3, 16:0 OH/18:2, 16:0 OH/18:1, 16:0/18:1 OH, 16:0 OH/18:0 OH, respectively (Table S1).

In the negative ionization mode, three forms of lipids were observed in lipid X, which were eluted at 19.78, 20.77, and 21.29 min. Each mass spectrum showed two ions with m/z values corresponding to $[M+HCOO]^-$ and $[M-H]^-$ ions of the molecules identified as No. **2**, **3,** and **4** by the positive ionization mode (Fig. S7). LC-MS characterization results for lipid X indicated that this novel lipid might be MGDG containing at least one ω1HFA moiety and either C16 or C18 FA, as generally existing in *Synechocystis* cells. The lower mobility in lipid X than in MGDG on the TLC plates might be caused by the higher possibility of hydrogen bond formation between a hydroxy group of the ω1HFA and silanol group (-Si-OH) on the TLC plate. This lower mobility of lipid X might also cause a lower ω1HFA ratio in galactolipids, i.e., MGDG and DGDG, than that

in SQDG and PG. LC-MS analysis revealed that lipid X might possess a 1:1 molecular ratio of ω1HFAs and standard FAs. These results indicated that MGDG in *aaKASIII*+/*phaC*−/*CphaAB*+ cells also contained ω1HFA. The introduction of 16:0 OH into the sn-2 position of lipids showed that MGDG contained a ω1HFAs ratio similar to that of PG and SQDG because FA at the sn-2 position is common to all lipid classes in *Synechocysitis*.

Table 1. Fatty acid composition of each lipid class in *Synechocystis* cells.

Strain	Lipid	Fatty acids							
	Class	16:0	18:0	18:1	18:2	18:3	16:0 OH	18:0 OH	18:1 OH
Wild type	MGDG	53.9 ± 3.0	1.7 ± 0.4	8.1 ± 5.3	17.6 ± 1.5	18.7 ± 0.7	-[a]	-	-
	DGDG	55.2 ± 4.4	3.9 ± 1.7	7.6 ± 1.7	21.2 ± 2.0	12.0 ± 6.0	-	-	-
	SQDG	68.9 ± 7.2	3.3 ± 1.8	11.9 ± 5.8	14.6 ± 1.0	1.3 ± 0.8	-	-	-
	PG	60.6 ± 5.7	6.9 ± 2.2	11.3 ± 2.3	24.4 ± 2.1	1.9 ± 1.2	-	-	-
	Total	48.0 ± 0.4	1.6 ± 0.2	12.3 ± 3.5	21.9 ± 2.0	16.2 ± 1.1	-	-	-
aaKASIII+/phaC−/CphaAB+	MGDG	50.3 ± 3.9	2.6 ± 1.0	12.1 ± 6.0	19.6 ± 1.4	15.5 ± 1.3	t[b]*	t*	t*
	DGDG	50.4 ± 1.5	4.6 ± 2.1	9.1 ± 1.8	20.9 ± 2.9	14.9 ± 0.9	0.1 ± 0.0*	-	t*
	SQDG	56.0 ± 1.5	5.4 ± 0.8	18.6 ± 4.5	18.6 ± 2.7	0.6 ± 0.1	0.5 ± 0.2	t	0.3 ± 0.1
	PG	51.1 ± 1.4	7.3 ± 3.8	15.2 ± 2.5	24.1± 1.7	1.5 ± 0.2	0.4 ± 0.1	t	0.5 ± 0.2
	Total	45.1 ± 0.8	3.3 ± 0.4	15.6 ± 4.3	22.2 ± 3.0	12.6 ± 1.6	0.6 ± 0.1	0.1 ± 0.0	0.7 ± 0.2

aaKASIII+/phaC−/CphaAB+; the cells in which the *fabH* gene was substituted with the *KASIII* gene from *Alicylobacillus acidocalderius*, and the *phaC* gene was substituted with the *phaAB* genes from *Cupriavidus necator* H16 driven by the *cpc* promoter.

MGDG; monogalactosyl diacylglycerol, DGDG; digalactosyl diacylglycerol, SQDG; sulfoquinovosyl diacylglycerol, PG; phosphatidyl diacylglucerol.

16:0; palmitic acid, 18:0; stearic acid, 18:1; oleic acid, 18:2; linoleic acid, 18:3; γ-linolenic acid, 16:0 OH; 15-hydroxy hexadecanoic acid, 18:0 OH; 17-hydroxy octadecanoic acid, 18:1 OH; 17-hydroxy octadic-9-enoic acid.

Data are averages of 3 replicates with the standard deviation.

[a]Not detected

[b]Trace amount (less than 0.04%)

*Significant difference was indicated by Student's *t*-test when compared with total lipid ($P < 0.05$)

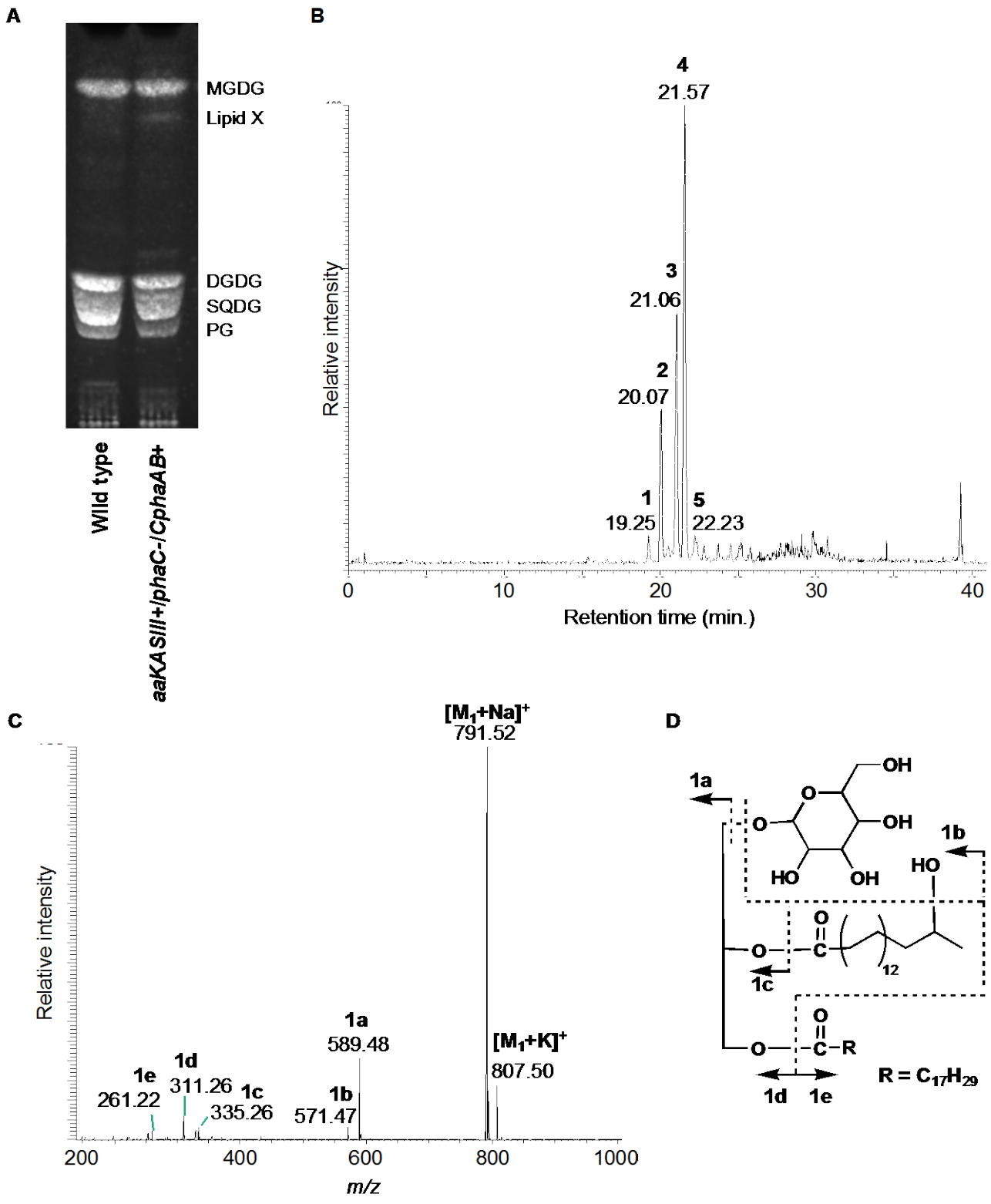

Fig. 5 (A) Thin-layer chromatography (TLC) analysis of lipid extracts from wild-type and *aaKASIII+/phaC−/CphaAB+*, the cells in which the *fabH* gene was substituted with the *KASIII* gene from *Alicylobacillus acidocalderius*, and the *phaC* gene was substituted with the *phaAB* genes from *Cupriavidus necator* H16 driven by the *cpc* promoter. Abbreviations of lipid classes on TLC are below: MGDG;

monogalactosyl diacylglycerol, DGDG; digalactosyl diacylglycerol, SQDG; sulfoquinovosyl diacylglycerol, PG; phosphatidyl diacylglucerol. (B) Base peak chromatograms obtained in the liquid chromatography-mass spectrometry (LC-MS) analysis of lipid X with positive ionization. (C) Mass spectra of peak 1 in positive ion mode. M_1 indicates lipid molecule. $[M_1+Na]^+$ and $[M_1+K]^+$ indicate sodium and potassium adduct ion, respectively. (D) The proposed molecular structure and fragmentation of peak **1**.

4 Conclusions

We succeeded in constructing the ω1HFA-producing cyanobacterial strain, which expresses the promiscuous KASIII from *A. acidocalderius* by substitution of the native KASIII gene and the exogenous PhaAB from *C. necator* H16 by substitution of the PHB synthetase gene. Under 70 μmol photons m^{-2} s^{-1}, this transformant produced 2.1 mol% of ω1HFAs in the total FAs and showed growth inhibition. In contrast, under 35 μmol photons m^{-2} s^{-1}, the mutant strain growth recovered to almost the same level as that of the wild-type strain. From the time-course experiment of the relationship between the ω1HFAs ratio and photosynthetic parameters such as photosynthetic activity, the quantum efficiency of PSII and chlorophyll content indicated that ω1HFA production inhibited the photosynthesis of *Synechocystis*. Lipid analysis of the mutant showed that galactoglycerolipids, which are MGDG and DGDG, contained a small amount of ω1HFAs compared to those of other lipids, and a novel spot appeared on TLC analysis, which contained ω1HFAs.

CRediT authorship contribution statement

Takashi Inada: Conceptualization, methodology, validation, formal analysis, investigation, writing - original draft, visualization. **Shuntaro Machida:** Methodology, investigation, resources. **Koichiro Awai:** Investigation resources. **Iwane Suzuki:** Conceptualization, methodology, resources, writing-review & editing, visualization, supervision, project administration, funding acquisition.

Acknowledgment

The strains of *A. acidocalderius* subsp. *acidocalderius* JCM 5260^T and *C. necator* H16 JCM 20644 were obtained from RIKEN BRC, which is a participant in the National BioResources Project of MEXT, Japan. This work was financially supported by JSPS KAKENHI Grant No. JP24119501.

Statement of Informed Consent, Human/Animal Rights

We did not apply any materials from Human and Animal in this study.

Reference

[1] U. Biermann, W. Friedt, S. Lang, W. Lühs, G. Machmüller, J.O. Metzger, M.R. Mark, H.J. Schäfer, M.P. Schneider, New syntheses with oils and fats as renewable raw materials for the chemical industry, Angew Chemie Int Ed. 39 (2000) 2206–2224. https://doi.org/10.1002/9783527619849.ch25.

[2] K.R. Kim, D.K. Oh, Production of hydroxy fatty acids by microbial fatty acid-hydroxylation enzymes, Biotechnol Adv. 31 (2013) 1473–1485. https://doi.org/10.1016/j.biotechadv.2013.07.004.

[3] A. V. Rawlings, Trends in stratum corneum research and the management of dry skin conditions, Int J Cosmet Sci. 25 (2003) 63–95. https://doi.org/10.1046/j.1467-2494.2003.00174.x.

[4] A. Abe, K. Sugiyama, Growth inhibition and apoptosis induction of human melanoma cells by ω-hydroxy fatty acids, Anticancer Drugs. 16 (2005) 543–549. https://journals.lww.com/anti-cancerdrugs/Abstract/2005/06000/Growth_inhibition_and_apoptosis_induction_of_human.10.aspx.

[5] C. Liu, F. Liu, J. Cai, W. Xie, T.E. Long, S.R. Turner, A. Lyons, R.A. Gross, Polymers from fatty acids: Poly(ω-hydroxyl tetradecanoic acid) synthesis and physico-mechanical studies, Biomacromolecules. 12 (2011) 3291–3298. https://doi.org/10.1021/bm2007554.

[6] M. Schrewe, A.O. Magnusson, C. Willrodt, B. Bühler, A. Schmid, Kinetic analysis of terminal and unactivated C-H bond oxyfunctionalization in fatty acid methyl esters by monooxygenase-based whole-cell biocatalysis, Adv Synth Catal. 353 (2011) 3485–3495. https://doi.org/10.1002/adsc.201100440.

[7] F. Pinot, Cytochrome P450 metabolizing fatty acids in living organisms, FEBS J. 278 (2011) 181–181. https://doi.org/10.1111/j.1742-4658.2010.07946.x.

[8] I.N.A. Van Bogaert, S. Groeneboer, K. Saerens, W. Soetaert, The role of cytochrome P450 monooxygenases in microbial fatty acid metabolism, FEBS J. 278 (2011) 206–221. https://doi.org/10.1111/j.1742-4658.2010.07949.x.

[9] H.A. Park, G. Park, W. Jeon, J.O. Ahn, Y.H. Yang, K.Y. Choi, Whole-cell biocatalysis using cytochrome P450 monooxygenases for biotransformation of sustainable bioresources (fatty acids, fatty alkanes, and aromatic amino acids), Biotechnol Adv. (2020) 107504. https://doi.org/10.1016/j.biotechadv.2020.107504.

[10] M. Kajikawa, T. Abe, K. Ifuku, K.I. Furutani, D. Yan, T. Okuda, A. Ando, S. Kishino, J. Ogawa, H. Fukuzawa, Production of ricinoleic acid-containing monoestolide triacylglycerides in an oleaginous diatom, Chaetoceros gracilis, Sci Rep. 6 (2016) 1–13. https://doi.org/10.1038/srep36809.

[11] R. Holic, H. Yazawa, H. Kumagai, H. Uemura, Engineered high content of ricinoleic acid in fission yeast Schizosaccharomyces pombe, Appl Genet Mol Biotechnol. 95 (2012) 179–187. https://doi.org/10.1007/s00253-012-3959-6.

[12] A. Kato, K. Use, N. Takatani, K. Ikeda, M. Matsuura, K. Kojima, M. Aichi, S.I. Maeda, T. Omata, Modulation of the balance of fatty acid production and secretion is crucial for enhancement of

growth and productivity of the engineered mutant of the cyanobacterium Synechococcus elongatus, Biotechnol Biofuels. 9 (2016) 91. https://doi.org/10.1186/s13068-016-0506-1.

[13] A.M. Ruffing, Improved free fatty acid production in cyanobacteria with Synechococcus sp. PCC 7002 as host, Front Bioeng Biotechnol. 2 (2014) 17. https://doi.org/10.3389/fbioe.2014.00017.

[14] X. Liu, J. Sheng, R. Curtiss, Fatty acid production in genetically modified cyanobacteria, Proc Natl Acad Sci U S A. 108 (2011) 6899–6904. https://doi.org/10.1073/pnas.1103014108.

[15] S. Machida, I. Suzuki, Characterization of cyanobacterial cells synthesizing 10-methyl stearic acid, Photosynth Res. 139 (2019) 173–183. https://doi.org/10.1007/s11120-018-0537-5.

[16] S. Machida, Y. Shiraiwa, I. Suzuki, Construction of a cyanobacterium synthesizing cyclopropane fatty acids, Biochim Biophys Acta Mol Cell Biol Lipids. 1861 (2016) 980–987. https://doi.org/10.1016/j.bbalip.2016.05.012.

[17] C.E. Drakontis, S. Amin, Biosurfactants: Formulations, properties, and applications, Curr Opin Colloid Interface Sci. 48 (2020) 77–90. https://doi.org/10.1016/j.cocis.2020.03.013.

[18] S. Garg, L. Rizhsky, H. Jin, X. Yu, F. Jing, M.D. Yandeau-Nelson, B.J. Nikolau, Microbial production of bi-functional molecules by diversification of the fatty acid pathway, Metab Eng. 35 (2016) 9–20. https://doi.org/10.1016/j.ymben.2016.01.003.

[19] K. Sudesh, K. Taguchi, Y. Doi, Effect of increased PHA synthase activity on polyhydroxyalkanoates biosynthesis in Synechocystis sp. PCC6803, Int J Biol Macromol. 30 (2002) 97–104. https://doi.org/10.1016/S0141-8130(02)00010-7.

[20] B. Wang, S. Pugh, D.R. Nielsen, W. Zhang, D.R. Meldrum, Engineering cyanobacteria for photosynthetic production of 3-hydroxybutyrate directly from CO2, Metab Eng. 16 (2013) 68–77. https://doi.org/10.1016/j.ymben.2013.01.001.

[21] J.G.K. Williams, Construction of specific mutations in photosystem II photosynthetic reaction center by genetic engineering methods in Synechocystis 6803, Methods Enzymol. 167 (1988) 766–778. https://doi.org/10.1016/0076-6879(88)67088-1.

[22] R.Y. Stanier, R. Kunisawa, M. Mandel, G. Cohen-Bazire, Purification and properties of unicellular blue-green algae (order Chroococcales)., Bacteriol Rev. 35 (1971) 171–205.

[23] M.N. Wada Hajime, Synechocystis PCC6803 mutants defective in desaturation of fatty acids, Plant Cell Physiol. (1989) 971–978. https://doi.org/10.1093/oxfordjournals.pcp.a077842.

[24] C. Yanisch-Perron, J. Vieira, J. Messing, Improved M13 phage cloning vectors and host strains: nucleotide sequences of the M13mpl8 and pUC19 vectors, Gene. 33 (1985) 103–119. https://doi.org/10.1016/0378-1119(85)90120-9.

[25] G. Bertani, Studies on lysogenesis. I. The mode of phage liberation by lysogenic Escherichia coli., J Bacteriol. 62 (1951) 293–300.

[26] T. Kotajima, Y. Shiraiwa, I. Suzuki, Functional screening of a novel Δ15 fatty acid desaturase from the coccolithophorid Emiliania huxleyi, Biochim Biophys Acta Mol Cell Biol Lipids. 1841 (2014) 1451–1458. https://doi.org/10.1016/j.bbalip.2014.07.010.

[27] N. Nicolaides, V.G. Soukup, E.C. Ruth, Mass spectrometric fragmentation patterns of the acetoxy and trimethylsilyl derivatives of all the positional isomers of the methyl hydroxypalmitates, Biol Mass Spectrom. 10 (1983) 441–449. https://doi.org/10.1002/bms.1200100802.

[28] K. Komagata, K.I. Suzuki, 4 Lipid and cell-wall analysis in bacterial systematics, Methods Microbiol. 19 (1988) 161–207. https://doi.org/10.1016/S0580-9517(08)70410-0.

[29] M. Kates, Techniques of lipidology, in: R. Burdon, P. van Knippenberg (Eds.), Lab. Tech. Biochem. Mol. Biol., 2nd ed., American Elsevier, New York, 1986: pp. 347–446. https://doi.org/10.1042/bst0160906.

[30] K. Awai, H. Ohta, N. Sato, Oxygenic photosynthesis without galactolipids, Proc Natl Acad Sci U S A. 111 (2014) 13571–13575. https://doi.org/10.1073/pnas.1403708111.

[31] N.T. de Marsac, J. Houmard, Complementary chromatic adaptation: physiological conditions and action spectra, Methods Enzymol. 167 (1988) 318–328. https://doi.org/10.1016/0076-6879(88)67037-6.

[32] B. Panda, P. Jain, L. Sharma, N. Mallick, Optimization of cultural and nutritional conditions for accumulation of poly-β-hydroxybutyrate in Synechocystis sp. PCC 6803, Bioresour Technol. 97 (2006) 1296–1301. https://doi.org/10.1016/j.biortech.2005.05.013.

[33] J. Liu, C. Zhang, W. Lu, Biosynthesis of long-chain ω-hydroxy fatty acids by engineered Saccharomyces cerevisiae, J Agric Food Chem. 67 (2019) 4545–4552. https://doi.org/10.1021/acs.jafc.9b00109.

[34] K. Kobayashi, K. Endo, H. Wada, Specific distribution of phosphatidylglycerol to photosystem complexes in the thylakoid membrane, Front Plant Sci. 8 (2017) 1991. https://doi.org/10.3389/fpls.2017.01991.

[35] K. Kobayashi, H. Wada, Role of lipids in chloroplast biogenesis, in: Subcell Biochem., Springer New York, 2016: pp. 103–125. https://doi.org/10.1007/978-3-319-25979-6_5.

[36] P. Sae-Tang, Y. Hihara, I. Yumoto, Y. Orikasa, H. Okuyama, Y. Nishiyama, Overexpressed superoxide dismutase and catalase act synergistically to protect the repair of psii during photoinhibition in synechococcus elongatus PCC 7942, Plant Cell Physiol. 57 (2016) 1899–1907. https://doi.org/10.1093/pcp/pcw110.

[37] J. Bhattacharya, K. GhoshDastidar, A. Chatterjee, M. Majee, A.L. Majumder, Synechocystis Fe superoxide dismutase gene confers oxidative stress tolerance to Escherichia coli, Biochem. Biophys. Res. Commun. 316 (2004) 540–544. https://doi.org/10.1016/j.bbrc.2004.02.084.

[38] R.V.V. Tatituri, M.B. Brenner, J. Turk, F.F. Hsu, Structural elucidation of diglycosyl diacylglycerol and monoglycosyl diacylglycerol from Streptococcus pneumoniae by multiple-stage linear ion-trap mass spectrometry with electrospray ionization, J Mass Spectrom. 47 (2012) 115–123. https://doi.org/10.1002/jms.2033.

[39] L.S. Pakkiri, B.A. Wolucka, E.J. Lubert, C.J. Waechter, Structural and topological studies on the lipid-mediated assembly of a membrane-associated lipomannan in Micrococcus luteus, Glycobiology. 14 (2004) 73–81. https://doi.org/10.1093/glycob/cwh012.

[40] O. Montero, Lipid profiling of Synechococcus sp. PCC7002 and two related strains by HPLC coupled to ESI-(Ion Trap)-MS/MS, Z Naturforsch C Biosci. 66 (2011) 0149. https://doi.org/10.5560/znc.2011.66c0149.